Stent Strut Detection by Classifying a Wide Set of IVUS Features

Rui Hua[1] *, Oriol Pujol[1], Francesco Ciompi[1], Simone Balocco[1], Marina Alberti[1], Fina Mauri[2], and Petia Radeva[1]

[1]Universitat de Barcelona, Barcelona, Spain
[2]Hospital Germans Trias i Pujol, Badalona, Spain

Abstract. Stent placement is a well-established clinical routine for treating coronary diseases due to its safety and minimal invasive surgery. In this paper, an automatic method for stent struct detection in Intravascular Ultrasound (IVUS) images is proposed based on a novel framework, which combines local and contextual information of strut appearance. In the first stage, local features are extracted from a wide filter base and used in a pixel-wise classification aimed at detecting candidate pixels belonging to stent struts. Since the appearance of the contextual surrounding structures is critical to remove artifacts with similar local appearance to struts, the former detection map is refined by using contextual features from the image patch centered at the candidate pixel.The proposed algorithm has been widely tested on 273 images of 12 pullbacks achieving encouraging results.

Keywords: IVUS analysis, stent strut detection, feature extraction

1 Introduction

Atherosclerosis is a hazardous disease, in which arterial wall hardens and thickens. A routine treatment for this kind of coronary artery disease is stent placement, which can re-dilate the artery with minimal invasive surgery. However, this technique also carries considerable potential risk due to underexpansion or malaposition of the stent, which can increase the risk of restenosis and thrombosis. IVUS is a catheter-based technique, which allows to visualize the result of stent vessel placement as well as to detect underexpansion and malaposition. Due to the large amount of data acquired during an IVUS pullback, manual analysis of stent positioning is difficult and time-consuming. Therefore, an automatic method for stent strut detection in IVUS images is on demand to speed up this analysis and reduce the subjectivity of manual segmentation [4].

Despite of the high clinical interest, surprisingly, only very little research on automatic analysis of stent implantation in IVUS can be found in the literature. Cañero et al. [1] proposed a technique to visualize and quantify the

* This work has been supported in part by the projects TIN2009-14404-C02 and CONSOLIDER-INGENIO CSD 2007-00018. We specially thank to Juan Rigla from BSCI for the valuable help and support.

mutual position between the stent and the vessel wall in IVUS pullbacks. Two deformable generalized cylinders, corresponding to the vessel wall and the stent, were adapted to image features in the IVUS sequence in order to obtain a 3D reconstruction of the stent and vessel borders. This algorithm showed its potential of detecting stent border, but it has only been qualitatively validated. Dijkstra et al. [4] proposed a stent contour detection algorithm. Firstly, a rough detection was performed to detect stent border based on brightness information. Then, two different model-guide optimizations were carried out to optimize the results. An improved method was proposed by the same authors [5], in which the local stent contour was adjusted using the information of the whole 3D model. This technique demonstrated its capability of detecting stent boundaries, however, it requires manual correction and images of good quality. A method for automatic detection of bio-absorbable coronary stent was proposed by Rotger et al. [8]. In this work, a cascade of classifiers was employed based on Haar-like features, which were selected to take advantage of the special appearance of polymer stent in IVUS images. This method is specialized on biodegradable struts and metallic struts are not considered by the authors.

In this paper, an automatic method is proposed to detect stent struts in 2D IVUS frames. The proposed detection method is mainly based on extraction of a wide set of IVUS features and applying machine learning techniques, due to the large amount of variation of the appearance of stents and complexity of IVUS images. The detection framework consists of two main stages. Firstly, pixel-wise descriptors are constructed and classified to detect potential strut candidates. This step is capable to locate almost all the struts, while still allowing some false positives (FPs). Secondly, these strut candidates are represented in a feature space using higher order contextual information by means of patch-based descriptors. Thus, stent struts are detected according to the morphological structures that surround them. Finally, the detection windows are merged to obtain an accurate strut location. We validate our method on 12 patients dataset of different clinical situations (underexpanded or malaposed stents, etc.) extracting several statistical measures like precision, sensitivity and F-measure to analyse the performance of the method.

2 Method

The pipeline of our method for automatic stent strut detection is shown in Fig.1.

2.1 Pixel-Based Classification

Stent struts appear in IVUS images as thin strips, which are bright and close to lumen, as shown in Fig.1 (a). Considering the intensity and shape characteristics of stent struts, several features have been specially chosen for the detection task. The intensity properties of stent struts are captured using: its intensity, the maximum, mean intensity and standard deviation of its neighbourhood. Besides, ridges are good at detecting connected regions of high intensities [1].

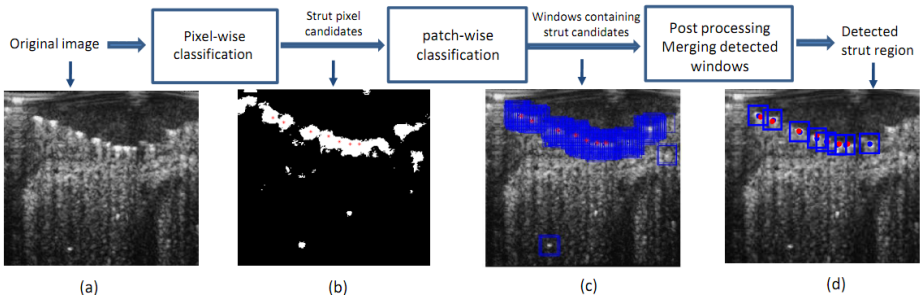

Fig. 1: Pipeline of the algorithm: (a) original image in polar system; (b) First strut detection map (c) Detected windows (blue) containing strut candidates; (d) Final detection windows in blue with their centers (blue dots) and ground truth (red dots).

In addition, the texture information of the image can be captured by 20 Gabor filters at different scales and orientations [2]. Furthermore, the shape of the struts is represented by a blob detector [6], which is a circularly symmetric Laplacian of Gaussian operator producing a high response at the center of image region with a blob shape. In summary, 36 local features are obtained to describe strut pixels.

Once defined the descriptor of strut centers, we proceed with a classification task to decide whether a pixel belongs to a strut. Adaboost with Decision Stumps is applied to the pixel-wise descriptors as one of the optimal classifiers to detect objects in images [9]. Moreover, it is capable of managing to learn from a large amount of data and features.

2.2 Patch-Based Classification

The first step produces potential strut candidates that represent a rough approximation of struts location. Since no contextual information has been exploited, the detection of false positives in regions characterized by high intensities and rounded shape is expected. In order to reduce FPs, a patch-based classification is defined, since the neighbourhood of stent struts provides a very diverse information to decide the presence of struts. Hence, we exploit the information of the local context around the strut candidates. For this purpose, a squared window of size (24×24) pixels is considered at each candidate pixel and a set of contextual features are extracted from each patch, as we estimated empirically that a window of (10×16) pixels (corresponding to (0.2×0.32) mm in polar coordinates) is enough to contain a strut. For each patch, three main operators are applied to extract features, namely Histogram of Oriented Gradients (HoG), Local Binary Patterns (LBP) and Steerable Filters (SF).

HoG is selected as a very characteristic descriptor, as it can capture the local appearance and shape of struts using the histogram of local gradient of different angles [3]. The edge structure related to image gradient can well characterize

local shape, as well as it is translation and intensity invariant. In this work, an image patch is divided into 3×3 overlapping cells and 9 orientation bins are used in the histogram as the optimal number of orientation bins for performance and computation cost [3]. LBP is another efficient texture descriptor, based on a binary comparison of the intensities of the center pixel and its neighbourhood. In this work, it is applied at the center of the image patch at 3 scales (circular neighbourhoods of radius of 1,2,3 pixels) and a rotationally invariant histogram is constructed for each of them achieving the property of being invariant to scale and rotation [7]. SF is used to highlight the strut regions. The image patch after filtering is divided into 9 parts, for each of which the mean and standard deviation are computed. Finally, the maximum intensity of the patch and the value of the distance with respect to the catheter are also included as additional features. A feature vector of length of 706 elements was extracted for each patch.

Adaboost with decision stumps is, again, chosen as the classifier to solve the binary classification problem to decide whether each detected window contains a struct or not.

2.3 Training Strategy

In order to train the pixel-wise classifier, a ground truth map needs to be generated to indicate which pixels belong to struts. As for this project only the center position of every strut is provided, the average size of the struts is measured by using an average template, which is calculated by taking a window of (36×36) pixels around every ground truth point and computing the average intensity of these windows.In order to select the real mean size of the struts, pixels with an intensity value lower than the 50% of the highest intensity are removed. However, the image contains a bright region below the center due to some mala-posed struts, therefore, as struts regions are symmetrical, the height is selected as twice the distance from the center to the uppermost point, achieving a size of (10×16) pixels. To ensure all the positive samples are taken from strut regions, a window (4×4) pixels is used instead. Negative samples are selected from outside the (10×16) window and pixels between these two windows are not considered for the training step.

2.4 Window Merging

The detection windows should be merged to reduce multiple candidates yield by the patch-wise classification. First of all, a window density image is generated by summing up the window number over each pixel in the image, as shown in Fig 2 (a). As stent struts often appear brighter than their neighbors, a combined density map is defined: $C = P \times I^3$, where $\times$ represents the pixel-wise product, P is the window density image, I is the image intensity. The regions with the highest response in the combined map are separated to locate precisely each strut, as shown in Fig.2. The result is further processed by removing very small regions and those, whose radius distance is further than 3/4 of the height of the image, taking into account the stent context in the IVUS image.

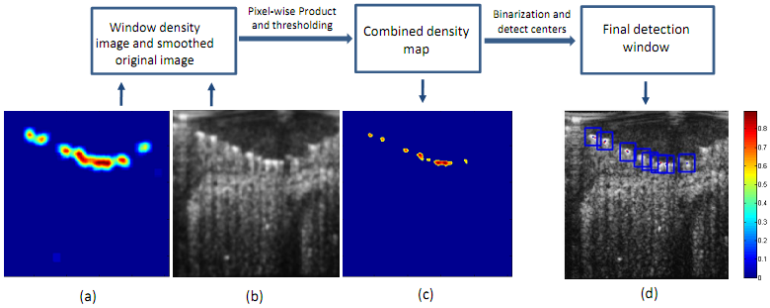

Fig. 2: Pipeline of window merging procedure: (a) Window density image; (b) Original image smoothed by a Gaussian; (c) Combined density map; (d) Final detection windows. (Red points are ground truth; Blue points are detected strut centers and blue windows are the final detection windows.)

3 Experimental Results

We validate our stent strut detection algorithm on 273 IVUS images from 12 pullbacks, in an average of 23 frames per pullback. These images contain stents from various companies, such as Skylor, Coroflex, and so on. All the images were acquired with Boston Scientific iLab IVUS Imaging System. In order to obtain a dataset of a large variability and of reasonable size, only around 23 representative frames are selected for each patient, considering the similarity of adjacent frames of one patient. As there is special clinical interest on under-expansion and mala-position, we have selected a challenging dataset, in which all the patients have under-expansion or mala-position to different degree and some patients have serious calcification. The ground truth was made by manually labelling the center of struts with a point by two physicians at Hospital Germans Trias i Pujol in Spain. Moreover, only the struts identified with high confidence were marked.

3.1 Evaluation methodology

In order to evaluate the detection result quantitatively, two measurements are computed. First, precision and sensitivity curves are given. Second, the average and standard deviation of the distance from a detected stent strut center to the ground truth center is reported. To decide whether a strut marked in the ground truth is correctly detected, for each detected strut center, we construct a square window of 10×16 pixels around it: if the ground truth point is inside the window, it is considered as a true positive (TP), otherwise it is considered as a FP. In order to compared our method with previous work, we also compute the F measure using precision and sensitivity, $F = PS/(P+S)$ [8].

Due to the large amount of data, the 12 patients were separated into 4 exclusive sets and cross validation has been applied on them. Given that 4-fold cross-validation 'leaving three patients out' is used to obtain the average score. Results

are expected to provide a lower bound on the performance of the methodology on new patients.

3.2 Results

The first quantitative analysis of the performance of the method is shown by the curve of precision and sensitivity of each patient varying with respect to the threshold of the combined window detection density map, as shown in Fig.3. The average equal precision and sensitivity, which is the crossing point between the two curves, is reached at 66% with an average threshold of 0.17.

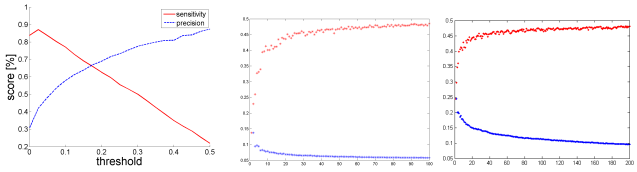

(a) (b) (c)

Fig. 3: (a) Curve of sensitivity (red) and precision (blue) varying with respect to the threshold of the combined map, averaged by the 4 folds of the cross validation. (b) Training error of Adaboost, strong classifier (red dots) and all the weak ones (blue dots), in the first classification. (c) Training error of Adaboost in the second classification.

In order to further measure the quality of the accuracy of the detection, the distance from the center of the detected struts to the ground truth was calculated. The average Euclidean distance is 2.18 pixels (0.04 mm) with a variance of 1.72 pixel (0.03 mm). Note that the average size of the stent struts is around 10×16 pixels, thus, our detection is extremely close to the ground truth.

Qualitative results are depicted in Fig. 4, where both the ground truth points and the results of the detection algorithm are shown. Most of the stent struts are correctly detected and the detections are very close to the ground truth points. Even, some of them can be argued to be more accurate, as they are closer to the real center of the strut than the ground truth points are. However, there remain some FPs. FPs usually corresponding to small calcified regions near the lumen border which have very similar appearance to stent struts. Additionally, we should note that physicians only annotated struts that they are completely confident about their presence. This causes some candidate struts (see Fig. 4(g)) to be considered as arguably false positives, worsening the overall performance. Missing struts mainly come from regions resembling fibrotic tissue. Fig. 4(h) shows an example of a malaposed strut that has been missed by the algorithm and can only be detected by considering the whole stent configuration.

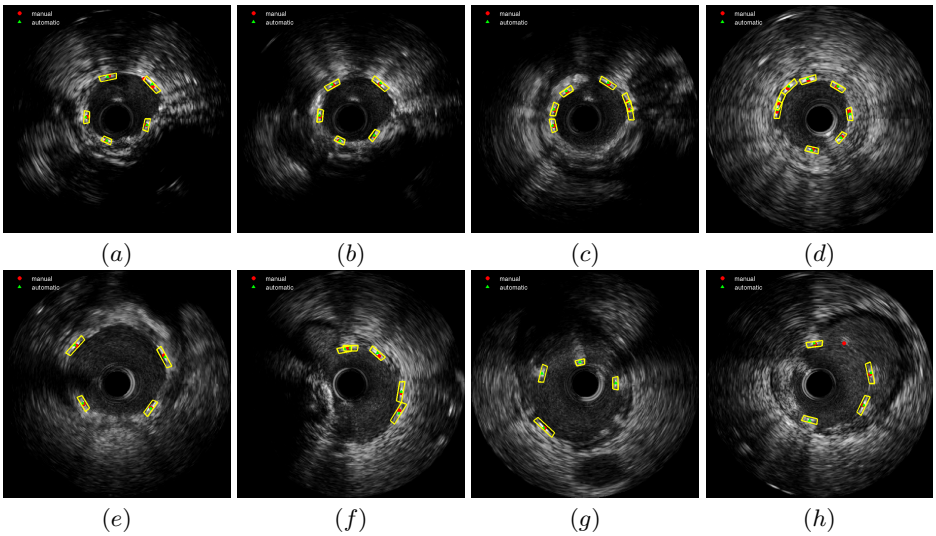

Fig. 4: Results of the automatic struts detection: The red points shows the ground truth; The green points present the detected strut centers and the yellow windows are the final detection windows

4 Discussions

In this work Adaboost was used with Decision Stumps as a reference classifier. The iteration limit in the first classification step is set to be 72, with which the error of Adaboost goes to less than 5%, as shown in Fig. 3 (a). This step ensures that nearly all positive samples are correctly detected but more than 90% of the whole set of pixels are removed. The second classifier focuses on the remaining candidate pixel set and describes the patches centred at them in order to capture the contextual appearance. This results in a 706-element feature vector. The second classifier converged at around 10% error rate Fig. 3 (b).

It is important to mention that in this dataset all the patients contain malaposition and some of them also have under-expansion. Images of patients with malaposition are challenging, since they have low intensities and they are not connected to the lumen, which may create a special shadow, different from normal struts.

5 Conclusions and Future Work

In this work, a novel method of stent strut detection is proposed, which integrates three steps: pixel-based local classification, patch-based feature extraction for contextual local appearance description and classification and, finally, a detection fusion step. The methodology is tested on a challenging dataset including

normal and malapposed stent struts. It is worth noting that malapposed stent struts have a different appearance from well-posed ones. This method is capable to detect struts with equal precision and sensitivity at 66% and an average pixel error of 2.18 pixels. In this paper we propose to validate the struts detection on 2D IVUS images without using any information of media, lumen or the whole pullback. Unfortunately there is no information in the literature on the performance of other methods working under the same conditions to compare with. Naturally, using global context like lumen and media as used by Rotger et.al. [8] or information from the whole pullback as used by Dijkstra et.al. [4] will additionally improve the results.

As discussed in the results section, there are some missing struts difficult to detect locally. Thus, one of the future lines is to include global morphological context information in order to disambiguate those cases. Additionally, very small calcified deposits on the lumen border resemble single stent struts need to be well handled. One of the main problems in assessing the results of the proposed method with respect to the state-of-the-art literature is the lack of a common database and methodology for automatic method validation. Different IVUS equipments and catheter specifications result in completely different problems. We plan to contribute in the future in constructing such a public database and well accepted validation methodology.

References

1. C. Canero, O. Pujol, and P. Radeva. et.al. Three-dimensional evaluation of the mutual position of stent and vessel via intracoronary ecography. In *Computer in Cardiology*, pages 265–268, 1999.
2. F. Ciompi. ECOC-based plaque classification using in-vivo and ex-vivo intravascular ultrasound data. Master's thesis, UAB, Spain, 2008.
3. N. Dalal and B. Triggs. Histograms of Oriented Gradients for Human Detection. In *Computer Vision and Pattern Recognition*, volume 1, pages 886–893, 2005.
4. J. Dijkstra and G. Koning. et. al. Automatic border detection in intravascular ultrasound images for quantitative measurements of the vessel, lumen and stent parameters. In *CARS*, volume 1230 of *ICS*, pages 916–922. Elsevier, 2001.
5. J. Dijkstra and G. Koning. et.al. Automatic stent border detection in intravascular ultrasound images. In *CARS*, pages 1111–1116, 2003.
6. T. Lindeberg. Detecting salient blob-like image structures and their scales with a scale-space primal sketch: A method for focus-of-attention. *IJCV*, 11:283–318, 1993.
7. T. Ojala, M. Pietikinen, and T. Menp. Multiresolution Gray-Scale and Rotation Invariant Texture Classification with Local Binary Patterns. *IEEE TPAMI*, 24:971–987, 2002.
8. D. Rotger, P. Radeva, and N. Bruining. Automatic detection of bioabsorbable coronary stents in ivus images using a cascade of classifiers. *IEEE Transactions TITB*, 14(2):535–537, 2010.
9. P. A. Viola and M. J. Jones. Robust real-time face detection. In *ICCV*, page 747, 2001.